Hydrol. Earth Syst. Sci. Discuss., 6, 1321–1345, 2009
www.hydrol-earth-syst-sci-discuss.net/6/1321/2009/

Hydrology and
Earth System
Sciences
Discussions

Analyzing influence of spatial resolution on the estimated evapotranspiration by using remote sensing data over an oasis area in Northwestern China

H. Tian[1], J. Wen[1], Z. B. Su[2], Y. M. Ma[3], L. Wang[1], X. K. Shi[1], R. Liu[1], T. T. Zhang[1], and J. H. Zhang[1]

[1]Laboratory for Climate Environment and Disasters of Western China, Cold and Arid Regions Environmental and Engineering Research Institute, Chinese Academy of Sciences, Lanzhou, Gansu 730000, China
[2]International Institute for Geo-information Science and Earth Observation (ITC), 7500 AA Enschede, The Netherlands
[3]Institute of Tibet Plateau Research, Chinese Academy of Sciences, Beijing 730000, China

Received: 26 December 2008 – Accepted: 16 January 2009 – Published: 27 February 2009

Correspondence to: J. Wen (jwen@lzb.ac.cn)

Published by Copernicus Publications on behalf of the European Geosciences Union.

Abstract

In this paper, the influence of spatial resolution on the precision of estimates was analyzed through evapotranspiration (ET hereafter) modeling over a typical oasis in Northwestern China by using the Landsat-TM and MODIS data. A relatively high consistency was observed between the TM-based latent heat flux and daily ET estimates and in-situ measurements, with relative errors of 9.7% and 8.8%, respectively. Despite lower precision of the relative errors of 22.4% and 17.0%, respectively, the MODIS-based latent heat flux and ET estimates can effectively depict the basic trend of the spatial distribution of the land surface processes. When the visible and near-infrared information of 250 m resolution was syncretized into MODIS LST retrieval algorithm, the precision of latent heat flux prediction was improved evidently. Additionally, the diurnal variation of the reference ET fraction shows that the temporal upscaling method of ET is suitable for the study area. In spite of suffering the influence of the heterogeneity of land surface, the moderate resolution MODIS data, combined with the parameterization model of land surface energy flux applied in this investigation, are suitable for the ET mapping at large scale while high-resolution data can serve as an important supplement.

1 Introduction

ET is one of the most important components of both the atmospheric and hydrological cycle. Together with rainfall and runoff, it controls the availability and distribution of water at the Earth's surface. For this reason, it is of significance to a number of water-related research and application areas (Rosenberg et al., 1983; Avissar, 1998; Bonan, 2002; Yunusa et al., 2004; Rana et al., 2005; Biggs et al., 2008). Information on ET reveals land-air feedback mechanisms and improves our understanding of energy and water cycles between the land and lower atmosphere. Over the latest few decades, there has been a focus on better determining ET and its spatial distribution by using satellite observations. Quantifying the spatial variability in latent heat flux and ET is more critical to water resource management in arid and semi-arid regions since basic weather and hydrology stations are spatially too sparse at discrete locations to effectively complete the ground-based estimation of ET.

At present, the land surface radiometric temperature observations are routinely available from sensors such as NOAA-AVHRR, EOS-MODIS or ENVISAT-MERIS/AATSR, and provide a unique spatially distributed boundary condition for land surface latent heat flux and ET modeling at regional scales. At the same time, a number of remote sensing ET schemes based on land surface energy balance principle have been applied widely (Norman et al., 1995; Bastiaanssen et al., 1998a, b; Kustas et al., 1999; Su, 2002). In virtue of high resolution satellite data, reliable flux estimates over heterogeneous landscape can be obtained. For example, a remote sensing parameterization model has been successfully applied over the cold and arid regions in the Western China and the heterogeneous landscape of the Jidda area of Saudi Arabia in Middle East (Wang et al., 1995, 1998; Ma et al., 2003, 2006a, b).

However, the applications of the model with coarse resolution satellite data, for instance, MODIS data, may result in significant errors in pixel-averaged fluxes and ET estimation over heterogeneous land surface, especially the arid and semiarid areas in the Western China since heterogeneity is the major feature of land surface here. Mountains, oases and deserts are the major land surface elements. Agriculture is mostly feasible by artificially supplying irrigation water because the annual precipitation is sparse. The main landscape of the arid region in the Northwestern China is representative for arid and semiarid agriculture areas where snowmelt water is the major source of irrigation. Despite the challenges of obtaining skillful retrievals, satellites observations are the only viable method for measuring the spatial variations in surface fluxes at regional scales. Determining effective techniques to make use of data from various sensors has been the focus of considerable research (Jackson, 1997; Kustas, 1990; Wan and Dozier, 1996), but little intercomparsions between sensors have been undertaken, with most analysis focused on individual satellite platforms. So there is few work in which the influences of spatial resolution of remote sensing data on estimation of land surface fluxes have been examined.

The presented investigation attempts to extend the previous researches in estimating surface heat fluxes from satellite observations over the arid region in Northwestern China. Its aims are outlined as follow:

- To derive different spatial resolution land surface temperatures and evaluate their performance over the heterogeneous area.
- A simple method will be introduced to scale-up the TM-based high resolution flux estimates to coarse resolution MODIS grids for the convenience of the intercomparsions between the ET estimates from different sensors' data.
- By verifying the characteristics of diurnal variation of the reference ET fraction, we intend to make sure that our temporal upscaling method of ET is authentic over the study area.
- To employ different spatial resolution remote sensing data to explore the influence of sensor's resolution on ET estimates. Two types of remote sensing data, Landsat-TM and Terra-MODIS data, will be used independently to derive land surface latent heat flux and ET based on the surface energy balance principle with vegetation and surface temperature information retrieved separately from each sensor. The ET estimates will be assessed against the ground-measured eddy covariance flux and the meteorological forcing data will be determined from the in-situ measurements coincident with satellite overpass times.
- To map the ET regional distribution at two spatial resolutions over the study area and check their overall trend through respective histograms. As the preliminary results of this investigation, the daily and monthly ET estimates over the whole Hei river basin will be given.

2 Description of the study area and data

To comprehend the energy and water cycle process of the oasis system, a mesoscale field observation experiment was conducted over the Jinta oasis from 5 June to 18 August 2004 (JTEX2004). This oasis, in a down-triangle form, is located in the middle reaches of the Hei river basin where is an arid inland river basin in the Northwestern China. The JTEX2004 study area, about 74 by 61 km^2 with a central location at 98.9° E/40.1° N, covers complex land surface types with various scales of artificially irrigated cropland (mainly growing wheat and cotton) and fence trees, dispersed along the river, canals, the sand desert and Gobi. The geographic location of JTEX2004 study area and observation sites (1∼8#) and deployed instruments are shown in Fig. 1.

During the JTEX2004 experiment, a large amount of data have been collected which are suitable for the study in energy and water cycles over the arid and semiarid regions. A subset of the surface radiation budget components, infrared (IR) radiation surface temperature, surface reflectance, air temperature, relative humidity and wind speed measured at the PAM and AWSs, turbulent fluxes measured by eddy covariance technique, soil heat flux of JTEX2004 data were applied to the parameterization of land surface latent heat flux and ET in this paper.

Terra-MODIS has 36 bands with 250 m resolution for visible and near-infrared bands 1 and 2, 500 m resolution for visible and near-infrared bands 3–7, and 1000 m resolution for twenty-nine visible, near-infrared and thermal-infrared bands 8–36. The Terra-MODIS images used in this study were at 10:30 LT (∼12:00 a.m. Beijing Standard Time – BST hereafter) during June to July 2004 over the JTEX2004 area (available at: http://ladsweb.nascom.nasa.gov./). In order to estimate ET over the JTEX2004 area, the Terra-MODIS land surface temperature, albedo and vegetation index products at 1000 m resolution were downloaded (available at: http://edcimswww.cr.usgs.gov/.).

Landsat-5 TM provides seven bands – 30 m resolution for three visible bands 1, 2 and 3, one near-infrared band 4, and two shortwave-infrared bands 5 and 7, 120 m resolution for thermal-infrared band 6. One TM image used in this study at 11:38 BST, 3 July 2004 over the JTEX04 area. The total shortwave broadband TM-albedo is derived from five atmospheric corrected narrowbands 1, 3, 4, 5 and 7 (Liang, 2001). TM-NDVI was derived from atmospheric corrected visible and near-infrared bands 3 and 4.

3 Theory and methodology

3.1 Model and its application

Based on the data collected during the Heihe River Field Experiment (HEIFE, 1988–1993), Wang and Ma proposed a remote sensing parameterization model for estimating land surface heat fluxes at regional scale (Wang et al., 1995, 1998; Ma et al., 1997, 2003, 2006a, b), in which the regional latent heat flux $\lambda E(x,y)$ can be derived as the residual of the energy budget theorem for land surface based on the condition of zero horizontal advection, i.e.

$$\lambda E(x,y) = R_n(x,y) - H(x,y) - G_O(x,y) \tag{1}$$

where the regional net radiation flux $R_n(x,y)$ can be expressed as

$$R_n = (1-\alpha_{\text{sfc}})\cdot K\downarrow + L\downarrow - \varepsilon_{\text{sfc}}\cdot\sigma\cdot T_{\text{sfc}}^4 \tag{2}$$

where the downwelling shortwave radiation component $K\downarrow$ and longwave radiation component $L\downarrow$ can take ground observed values. α_{sfc} and T_{sfc} are the land surface albedo and land surface temperature. The surface emissivity ε_{sfc} can be derived from vegetation coverage P_v (Valor and Caselles, 1996) as below

$$\varepsilon_{\text{sfc}} = \varepsilon_{\text{veg}}\cdot P_v + \varepsilon_{\text{soil}}\cdot(1-P_v) + 4\cdot d\varepsilon\cdot(1-P_v)\cdot P_v \tag{3}$$

where ε_{veg} and $\varepsilon_{\text{soil}}$ are the surface emissivities for full vegetation and bare soil, respectively, $d\varepsilon$ is the error item, and vegetation coverage (Carlson and Ripley, 1997) is obtained as

$$P_v = \left[\frac{\mathrm{NDVI} - \mathrm{NDVI}_{\mathrm{min}}}{\mathrm{NDVI}_{\mathrm{max}} - \mathrm{NDVI}_{\mathrm{min}}}\right]^2 \tag{4}$$

where $\mathrm{NDVI}_{\mathrm{max}}$ and $\mathrm{NDVI}_{\mathrm{min}}$ are the NDVI (Normalized Difference Vegetation Index) values for bare soil and full vegetation, respectively.

The regional distribution of sensible heat flux is calculated from

$$H(x,y) = \rho C_P \frac{T_{\mathrm{sfc}}(x,y) - T_a\,(x,y)}{r_a\,(x,y)} \tag{5}$$

where r_a is aerodynamic resistance, $T_a(x,y)$ is the regional distribution of air temperature at the reference height and can be derived from an interpolation method (Ma et al., 2003, 2006a, b).

The regional soil heat flux $G_O(x,y)$ is parameterized from following equation (Ma et al., 1997)

$$G_O(x,y)/R_n = \frac{T_{\mathrm{sfc}}}{\alpha_{\mathrm{sfc}}}\left[0.0032\alpha_{\mathrm{sfc}} + 0.0062\alpha_{\mathrm{sfc}}^2\right]\left[1 - 0.978\mathrm{NDVI}^4\right] \tag{6}$$

It should be mentioned that this model has a good performance when applied to the arid and cold regions and it can estimate latent heat flux with Landsat-TM data by a MAPD (the mean absolute percent difference) of 9.8% between the derived results and ground measured values at the HEIFE site (Ma et al., 2003), and by a APD (the absolute percent difference) of 9.7% in winter and of 9.9% in summer over the central Tibetan Plateau area (Ma et al., 2006a). It can even derive regional latent heat flux by a MAPD of 5.18% with landsat-7 ETM data over the Jiddah area of Saudi Arabia (Ma et al., 2006b). This study will use the parameterization model to derive land surface latent heat flux.

3.2 Upscaling the TM estimates to the MODIS grids

A preponderance of high spatial resolution Landsat-TM sensor in the Earth-observation scope is that it can depict the Earth's surface state or its changes in a more meticulous manner, particularly over the heterogeneous landscape, compared with moderate resolution MODIS sensor. But it measures the Eearth's surface in a 16 days repeat period, which means it can't produce images everyday over the same region as MODIS does. In addition, the visual and near-infrared (VIS/NIR) bands in these two sensors have the higher spatial resolution than the thermal-infrared (TIR) ones. Given no variation in the land surface state within a short period, the high resolution LST regional distribution temporally synchronizing with the MODIS data can be simulated by combining the TM visual and near-infrared bands' information with the ground-measured infrared (IR) surface temperatures over different landcover types.

In this paper, one scene of Landsat-5 TM image covering the study area at 11:38 BST, 3 July 2004, was used to estimate the regional LST at 30 m resolution at 12:10 BST, 4 July 2004 (i.e. the day's MODIS overpassing time). In this way, the land surface latent heat flux and ET estimates from the temporally synchronized but different resolution remote sensing data can be directly compared. In the first step, it is assumed that the NDVI regional distribution over the study area keeps invariant at least during several days. Over the inhomogeneous landscape, a 30 m pixel of TM VIS/NIR bands is simply considered as being composed of the vegetation and bare soil elements, respectively. The pixel-averaged land surface temperature $\overline{T}$ falls into two components, i.e. vegetation temperature T_{veg} and bare soil temperature T_{soil}. The mixed-pixel average surface temperatures $\overline{T}$ meet following relationship

$$\overline{\varepsilon} \cdot \sigma \cdot \overline{T}^{\,4} = (1 - P_v) \cdot \varepsilon_{\text{soil}} \cdot \sigma \cdot T_{\text{soil}}^4 + P_v \cdot \varepsilon_{\text{veg}} \cdot \sigma \cdot T_{\text{veg}}^4 \qquad (7)$$

where the pixel-averaged emissivity $\overline{\varepsilon}$ can be derived from the Eq. (3). The average vegetation coverage fraction of the mixed-pixel can be obtained with the Eq. (4). Both T_{veg} and T_{soil} at different landcover types can be obtained from the ground-measured

IR surface temperatures with the aid of the existing landcover map and the apriori knowledge of the landuse over the study area from in-situ investigations. Note that T_{veg} and T_{soil} have different diurnal variations in different days. The values of $\varepsilon_{\mathrm{veg}}$ and $\varepsilon_{\mathrm{soil}}$ at different landcover types can be acquired from MODIS emissivity spectral library (available at: http://www.icess.ucsb.edu/modis/EMIS/html/em.html). Then $\overline{T}$ (hereafter called TM30m LST) can be resolved from the Eq. (7).

In the second step, the latent heat flux and daily ET estimated from the simulated “TM30m” LST are upscaled to the MODIS 1 km grids in order to explore the influence of spatial resolution of the remote sensing data on land surface flux estimates. Here, a simple upscaling method of the spatial data is used and the pixel-averaged variable $\overline{f_{\text{mixed pixel}}}$ in a coarse MODIS 1 km grid is the integration consequence of the values f_i of all subpixel elements at 30 m resolution

$$\overline{f_{\text{mixed pixel}}} = \sum_i (S_i f_i) \tag{8}$$

where S_i is the area fraction of the number i subpixel and f_i is the subpixel-averaged value of land surface variable f. In fact, the Eq. (8) reflects the relationship between land surface variables at different scales.

3.3 Improvement of the MODST-LST retrieval

Two 250 m MODIS bands (VIS-band 1 and NIR-band 2) are syncretized into an operational MODIS-LST retrieval algorithm (Mao et al., 2005) in order to improve the retrieval precision. In this algorithm, LST is given as follow

$$T_s = [C_{32}(B_{31} + D_{31}) - C_{31}(D_{32} + B_{32})]/(C_{32}A_{31} - C_{31}A_{32}) \tag{9}$$

where $I_j = f(\varepsilon_j, \tau_j, T_j), (I = A, B, C, D; j = 31, 32)$, and T, ε, τ are the bright temperature, emissivity and atmospheric transmittance in the band j, respectively. The atmospheric transmittances in band 31 and band 32 are derived from the atmospheric water vapor content which can be retrieved from the apparent reflectances in MODIS band 2 and band 19 by utilizing a method proposed by Kaufman et al (Kaufman et al., 1992)

$$w = (\alpha - \ln \tau_w/\beta)^2, \quad \tau_w(19/2) = \frac{\mathrm{ref}_{19}}{\mathrm{ref}_2} \tag{10}$$

where the parameters α=0.02 and β=0.651 respectively over mixed land surface, otherwise setting α=0.012, β=0.651 over the full vegetation surface or α=−0.04, β=0.651 over the bare soil surface, respectively.

In the algorithm, the 250 m resolution of band 1 and band 2 (band1 was used to get NDVI) is kept and the 1 km resolution of band 19, band 31 and band 32 is resized to 250 m grid. In this way, the MODIS-LSTs at pseudo 250 m resolution can be retrieved to ameliorate the performance of MODIS LST algorithm and finally improve the precision of ET estimate by using MODIS data over the heterogeneous landscape.

3.4 Temporal upscaling of ET

The retrieved latent heat flux needs to be extrapolated to a daily ET serving for water resource management or as input for hydrologic model. In this paper the METRIC (*M*apping *E*vapo*T*ranspiration at high *R*esolution with *I*nternalized *C*alibration) model, a temporal upscaling method of ET developed by University of Idaho, USA (Allen et al., 2005) was deployed. In METRIC model, the reference ET fraction $\mathrm{EF}_{\mathrm{ref}}$, i.e. the ratio of actual ET to reference ET, should be introduced at first as constant during the whole daytime. Then, a time-averaged $\mathrm{EF}_{\mathrm{ref}}$ during a 10 min or 1 h period will be considered as the daily average $\mathrm{EF}_{\mathrm{ref}}$ in order to acquire the daily ET

$$\mathrm{ET}_{\mathrm{day}} = \mathrm{EF}_{\mathrm{ref}} \times \mathrm{ET}_{\mathrm{ref,day}} \tag{11}$$

where $\mathrm{ET}_{\mathrm{ref,day}}$, the daily reference ET, is calculated by the FAO-56 Penmen-Monteith equation (Allen et al., 1998), which is convenient for acquiring the regional reference ET at different time scales, such as 1 h or 1 day, only using the routine meteorology data.

4 Validation of the results and discussion

4.1 The intercomparsion between 1 km and 250 m MODIS-LSTs

The 1 km resolution MODIS LST product were compared with the ground-measured IR surface temperatures (ground-based measurements hereinafter called ground truth) at 1#, 4# and 8# observation sites (Fig. 2a). The Root Mean Square Error (RMSE) between MODIS LSTs and the ground truth at 4# site in homogeneous sandy desert is the least, and the RMSE at 1# site is almost twice high as the ones at 8# site. 1# site is at the east edge of Jinta oasis where underlying surface is a mixture of wheat cropland and sandy land whereas 8# site is at the densest and uniform cropland over Jinta oasis. It is evident that the discrepances of MODIS LSTs from the ground truth are variable under different underlying surface types. As the key input data for the model introduced in Sect. 3.1, the variation in the performance of MODIS-LSTs may bring on the decrease in the precision of land surface flux and ET estimates.

It is seen that the landsurface's thermodynamic state can be more factually depicted by the 250 m LSTs, compared with 1 km ones (Fig. 2b). The retrieval precision is significantly improved over the patchy oasis surface at 1# observation site and only lightly changed over the uniform underlying surface at 3# and 4# sites (the flat desert) and 8# site (the dense cropland). So it is expected that land surface fluxes estimated from 250 m LSTs will have a better precision than those from 1 km LSTs.

4.2 The diurnal variation of the reference ET fraction

By using hourly turbulent flux data measured by the eddy covariance system and meteorological variables by Automatic Weather Station (AWS) at 5# oasis observation site during the JTEX2004 from 29 June to 4 July, 2004, the hourly averaged reference ET fractions EF_{ref} in the same period were computed and presented (Fig. 3).

It is seen that the reference ET fractions reach a steady during the daytime, and have a considerable variation around sunrise and sunset (Fig. 3). Although they are very small at night and had a big fluctuation during 24 h, the daytime-averaged EF_{ref} is able to denote the daily average value, since the actual ET (integrated area under curve in Fig. 4) during nighttime only accounted for very small percentage of daily amount. For example, the integrals of latent heat flux observed at 1# and 5# sites before 7:00 LT and after 19:00 LT in 4 July 2004 only accounted for 5.4% and 3.5% of the total daily amount, respectively. Generally EF_{ref} is constant in the daytime (8:00∼18:00 LT), so an EF_{ref} observed or calculated during a short period of time such as 1 h in the daytime, particularly around midday, can serve as a 24-h-averaged ones for daily ET estimate. So the temporal up-scaling method of ET introduced in Sect. 3.4 is feasible over the study area.

4.3 The intercomparsion between ETs estimated from different spatial resolution data

The regional latent heat flux and daily ET at 30 m and 1 km spatial resolution, respectively were modelled independently from the scheme introduced in Sects. 3.1 and 3.4 by combining TM30m LST resulting from the method introduced in Sect. 3.2 and 1 km MODIS LST (MODIS1km hereafter), respectively with the routine meteorology data over the study area. Then TM30m variables, including LST, latent heat flux, reference ET fraction and daily ET were aggregated to 1 km spatial grids (TA1km hereafter) through Eq. (8) and furthermore compared with the corresponding MODIS1km variables.

The contrasts between the derived results and ground truths over the fragmentary oasis underlying surface at #1 and 5# observation sites are given (Fig. 4). It is found that MODIS1km LSTs are greater than the ground truth evidently, which reveals the notable mixed-pixel average effect associated with moderate resolution data (Fig. 4a). And TM30m LSTs are very close to the ground truth since the 30 m grids maybe contain relatively simplex land surface elements. The discrepance between TA1km LSTs and ground truth is obviously close to that between MODIS1km LSTs and ground truth, which displays that Eq. (8) can simulate the mixed-pixel average variable relatively well. It is seen that the model in Sect. 3.1 is reliable in that the relative error (RE) of TM30m latent heat flux is only 9.7% (Fig. 4b). But the flux prediction accuracy is reduced by the coarse resolution MODIS data, and the discrepance of MODIS1km flux from ground truth doubles that between TM30m flux and ground truth on the same type of underlying surface. At the same time, the discrepance between the TA1km and MODIS1km latent heat flux estimate is obviously less than that between TM30m and MODIS1km estimates; Moreover, the TA1km reference ET fraction and daily ET behave like the corresponding MODIS1km ones (Fig. 4c and d), both are obviously less than their ground truth. The discrepance between the MODIS1km results and ground truth is about two times as that of the TM30m results, which suggests that the spatial resolution of remote sensing data can significantly affect land surface flux estimation, particularly over heterogeneous landscape.

It is seen that the precision of the land surface latent heat flux derived from the algorithm-ameliorated 250 m MODIS-LST has a significant improvement compared with the MODIS1km estimates (Figs. 4b and 5). The Mean Absolute Percent Difference $\left(\mathrm{MAPD}=\frac{100}{n}\sum_{i=1}^{n}\left|\frac{x_{\mathrm{derived}}-x_{\mathrm{measured}}}{x_{\mathrm{measured}}}\right|\right)$ between the estimates and ground truth equals to 18.2%. Of course, the influence of heterogeneity of the land surface on flux prediction is still in presence, but it has been weaken to a visible degree.

So, it is clear that MODIS1km data may inevitably underestimate land surface latent flux over heterogeneous landscape but high resolution satellite data can suffer lesser influence of the heterogeneous landscape.

The regional distribution of the modelled TM30m and MODIS1km latent heat flux and daily ET over Jinta oasis and the corresponding histograms are shown in Figs. 6 and 7, respectively. It is seen that the high resolution remote sensing data can describe in detail the water and heat exchange process between the inhomogeneous land surface and atmosphere, whereas the moderate resolution data can give the right trend of the spatial distribution of the underlying surface fluxes and exhibit their advantage at the ET mapping at large scales.

Since high resolution remote sensing data such as ASTER and Landsat-TM/ETM are not always available due to their longer repeat period, it is a better alternative to adequately make use of everyday available MODIS data to meet the needs of real-time monitoring earth environment. Therefore the estimation of regional daily ET over Hei river basin was undertaken by utilizing Terra-MODIS 1 km data, and as the preliminary results of this work, the regional distribution maps of the daily ET under typical clear sky and total month ET amount over the whole Hei river basin are shown in Fig. 8.

5 Conclusions

In this paper we assessed the effect of pixel resolution on the estimation of ET by using different resolution (30 m Landsat-TM, 1 km Terra-MODIS) remote sensing data. The good agreements between the Landsat-based retrievals and in-situ measurements were found. The derived TM30m latent heat flux and ET, respectively, have about half of the same discrepances from the ground truths as those of the corresponding estimates by using coarse resolution MODIS1km data over the same type of underlying surface. Considering the complex spatial structure of the land surface over the study area, we think that TM data hold much promise for high-resolution and thus reliable flux mapping. Meanwhile both the land surface latent heat flux and ET may be underestimated by MODIS 1 km data due to the "average" response of MODIS sensor on land surface properties over the region with strong spatial variation of landscape. With the aid of routine meteorological data, the estimation of daily ET has a higher accuracy than latent heat flux prediction (Fig. 4b and d), and this improvement of precision of flux prediction is more obvious for coarse resolution data than for high resolution data. Because of the considerable influence of the spatial resolution of remote sensing data on modeling land surface processes, it is naturally expected that the precision of the latent heat flux estimates from the algorithm-ameliorated 250 m MODIS-LSTs has an evident improvement and in fact such estimates with a MAPD of 18.2% from the ground truth were obtained finally.

Usually, there is a gap between the desired resolution and the acceptable cost of remote sensing images, and high-resolution sensors are generally provided with a longer repeat period and thus the lower temporal resolution than moderate-resolution sensor, which constrains to a large degree the availability and application of high-resolution data. The moderate resolution data can depict the right trend of the spatial distribution of the underlying surface processes and exhibit their advantage at the regional ET prediction. So it is concluded that MODIS data are still acceptable and even more suitable for mapping the spatial distribution of ET or monitoring other environmental changes at continental or global scales while high-resolution Landsat-TM/ETM and EOS-ASTER data can serve as an important supplement.

References

Allen, R. G., Pereira, L. S., Raes, D., and Smith., M.: Crop Evapotranspiration: Guidelines for computing crop water requirements, Irrigation and Drainage Paper 56, Food and Agriculture Organization of the United Nations, Rome, 1998.

Allen, R. G., Tasumi, M., Trezza, R., Bastiaanssen, W., Morse, T., Kramber, W., and Wright, J.: METRIC: High Resolution Satellite Quantification of Evapotranspiration – Summary, University of Idaho, Kimberly, Idaho, USA, 94 pp., http://www.kimberly.uidaho.edu/water/metric/FtCollins/Allen_Ft_Collins_METRIC_Summary_7.pdf, 2005.

Avissar, R.: Which type of soil-vegetation-atmosphere transfer scheme is needed for general circulation models: a proposal for a higher-order scheme, J. Hydrol., 212–213, 136–154, 1998.

Bastiaanssen, W. G. M., Menenti., M., Feddesb, R. A., and Holtslag, A. A. M.: A remote sensing surface energy balance algorithm for land (SEBAL): 1. Formulation, J. Hydrol., 212–213, 198–212, 1998a.

Bastiaanssen, W. G. M., Pelgrum, H., Wang, J., Ma, Y. M., Moreno, J. F., Roerink, G. J., and Van der Wal, T.: Remote sensing surface energy balance algorithm for land (SEBAL): 2. Validation, J. Hydrol., 212–213, 213–229, 1998b.

Biggs, T. W., Mishra, P. K., and Turral, H.: Evapotranspiration and regional probabilities of soil moisture stress in rainfed crops, southern India, Agr. Forest Meteorol., 148, 1585–1597, 2008.

Bonan, G. B.: Hydrologic cycle, in: Ecological climatology: concepts and applications, Cambridge University Press, New York, 129–166, 2002.

Carlson, T. N. and Ripley, D. A.: On the relation between NDVI, fractional vegetation cover, and leaf area index, Remote Sens. Environ., 62, 241–252, 1997.

Jackson, T. J.: Soil moisture estimation using special satellite microwave imager satellite data over a grassland region, Water Resour. Res., 33, 1475–1484, 1997.

Kaufman, Y. J. and Gao, B. C.: Remote sensing of water vapor in the near IR from EOS/MODIS, IEEE T. Geosci. Remote, 5, 871–884, 1992.

Kustas, W. P.: Estimates of evapotranspiration with a one- and two-layer model of heat transfer over partial canopy cover, J. Appl. Meteorol., 29, 704–715, 1990.

Kustas, W. P. and Norman, J. M.: Evaluation of soil and vegetation heat flux predictions using a simple two-source model with radiometric temperature for partial canopy cover, Agr. Forest Meteorol., 94, 13–29, 1999.

Liang, S.: Narrowband to broadband conversions of land surface albedo, Remote Sens. Environ., 76, 213–238, 2001.

Ma, Y. M., Wang, J. M., Menenti, M., and Bastiaanssen, W. G. M.: The study of regional surface heat fluxes over the heterogeneous landscape of HEIFE, Climatic and Environmental Research (in Chinese), 2, 239–301, 1997.

Ma, Y. M., Ishikawa, H., Tsukamoto, O., Menenti, M., Su, Z., Yao, T. D., Koike, T., and Yasunari, T.: Determination of regional land surface heat flux densities over heterogeneous landscape of HEIFE integrating satellite remote sensing with field observations, J. Meteorol. Soc. Jpn., 80, 485–501, 2003.

Ma, Y. M., Zhong, L., Su, Z., Ishikawa, H., Menenti, M., and Koike, T.: Determination of regional distributions and seasonal variations of land surface heat fluxes from Landsat-7 Enhanced Thematic Mapper data over the central Tibetan Plateau area, J. Geophys. Res., 111, D10305, doi:10.1029/2005JD006742, 2006a.

Ma, Y. M., Tian, H., Ishikawa, H., Ohba, R., Ueda, H., and Wen, J.: Determination of regional land surface heat fluxes over a heterogeneous landsacpe of the Jiddah area of Saudi Arabia by using Landsat-7 ETM data, Hydrol. Process., 21, 1892–1900, 2006b.

Mao, K., Qin, Z., Shi, J., and Gong, P.: A practical split-window algorithm for retrieving land-surface temperature from MODIS data, Int. J. Remote Sens., 26, 3181–3204, 2005.

Norman, J. M., Kustas, W. P., and Humes, K. S.: Source approach for estimating soil and vegetation energy flux in observations of directional radiometric surface temperature, Agr.

Forest Meteorol., 77, 263–293, 1995.

Rana, G., Katerji, N., and Lorenzi, F.: Measurement and modelling of evapotranspiration of irrigated citrus orchard under Mediterranean conditions, Agr. Forest Meteorol., 128, 199–209, 2005.

Rosenberg, N. J., Blad, B. L., and Verma, S. B.: Microclimate – The Biological Environment of Plants, 2nd Ed., John Wiley & Sons, New York, 495, 1983.

Su, Z. B.: The Surface Energy Balance System (SEBS) for estimation of turbulent heat fluxes, Hydrol. Earth Syst. Sci., 6, 85–100, 2002, http://www.hydrol-earth-syst-sci.net/6/85/2002/.

Valor, E. V. and Caslles, V.: Mapping land surface emissivity from NDVI: Application to European, African, and South American areas, Remote Sens. Environ., 57, 167–184, 1996.

Wan, Z. and Dozier, J.: A generalized split-window algorithm for retrieving land-surface temperature from space, IEEE T. Geosci. Remote, 34, 832–905, 1996.

Wang, J., Ma, Y., Menenti, M., Bastiaanssen, W. G. M., and Mitsuta, Y.: The scaling-up of processes in the heterogeneous landscape of HEIFE with the aid of satellite remote sensing, J. Meteorol. Soc. Jpn., 73, 1235–1244, 1995.

Wang, J., Bastiaanssen, W. G. M., Ma, Y. M., and Pelgrum, H.: Aggregation of land surface parameters in the oasis-desert systems of North-west China, Hydrol. Process., 12, 2133–2147, 1998.

Yunusa, I. A. M., Walker, R. R., and Lu, P.: Evapotranspiration components from energy balance, sapflow and microlysimetry techniques for an irrigated vineyard in inland Australia, Agr. Forest Meteorol., 127, 93–107, 2004.

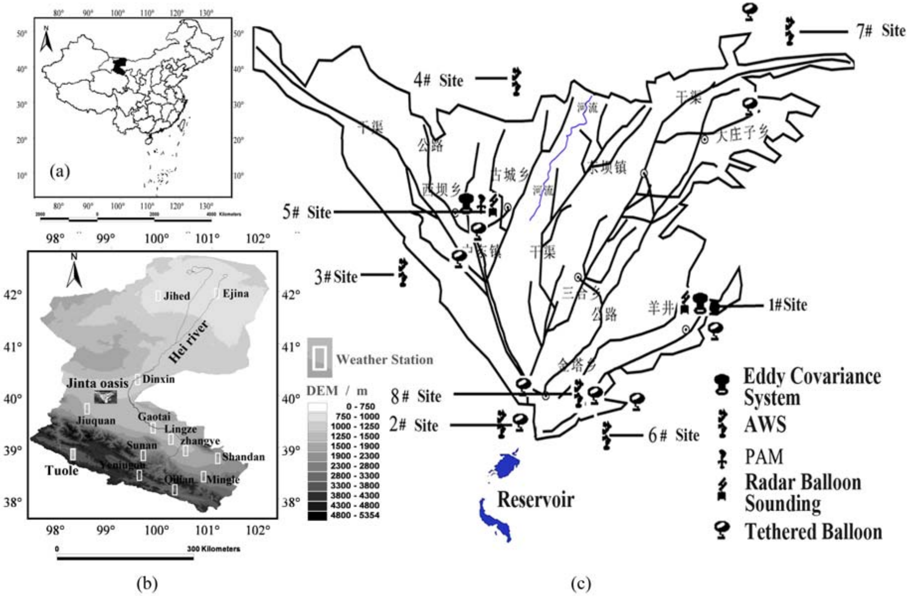

Fig. 1. **(a)** Geographic location of the Hei river basin, **(b)** Topography and location of weather stations over the Hei river basin, **(c)** Observation sites and instruments disposed during “JTEX2004” experiment.

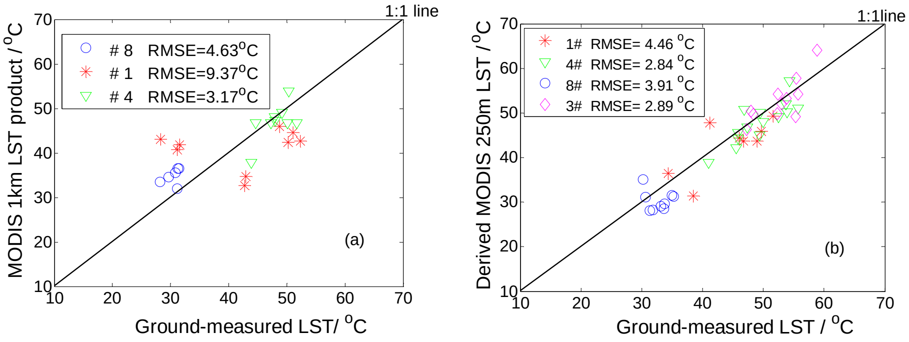

Fig. 2. The discrepancy between the ground-measured IR surface temperatures and **(a)** 1 km MODIS-LSTs **(b)** improved 250 m MODIS-LSTs.

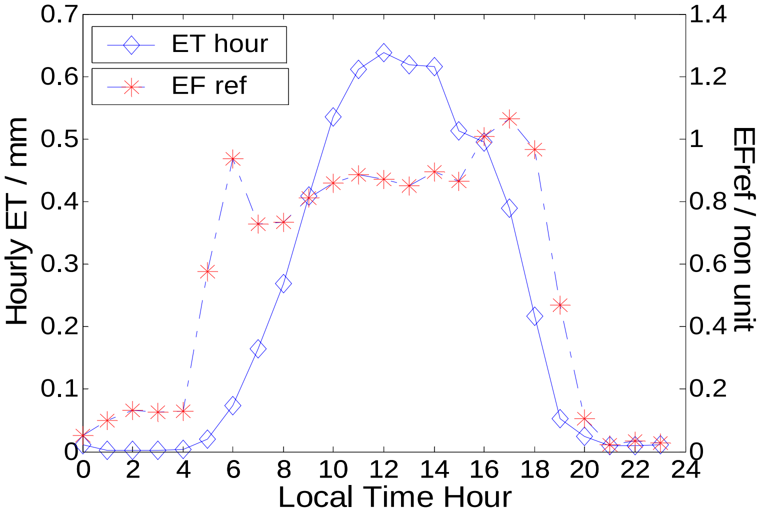

Fig. 3. Diurnal variation of the reference ET fraction at 5# observation site in the Jinta oasis.

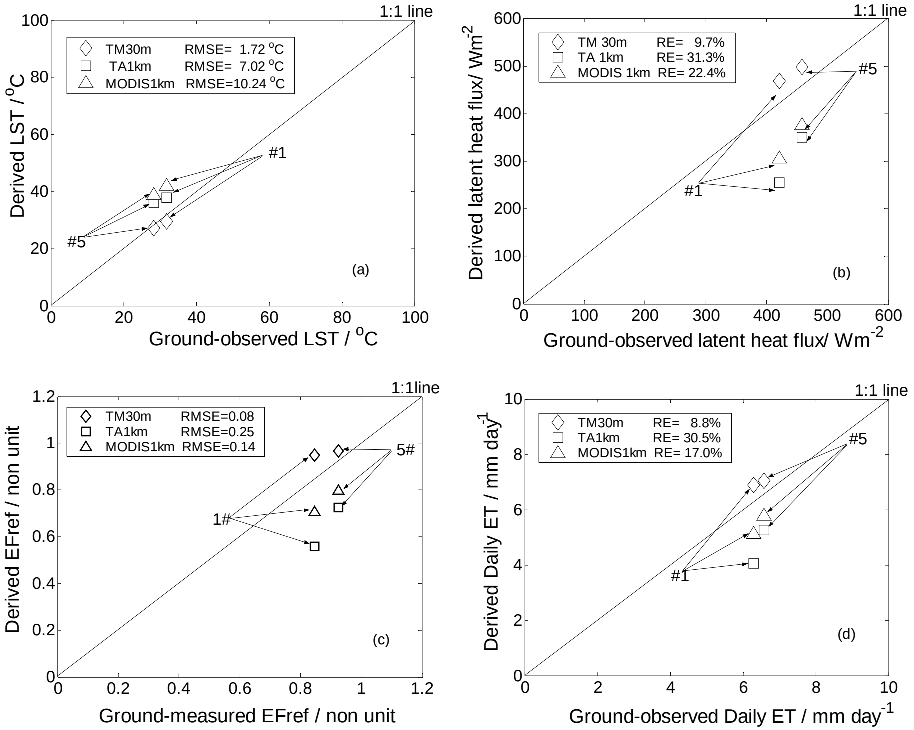

Fig. 4. The discrepance between the ground truth and **(a)** land surface temperature, **(b)** latent heat flux, **(c)** reference ET fraction, **(d)** daily ET estimated from different spatial resolution remote sensing data in 4 July 2004 at observation sites of “JTEX2004” experiment.

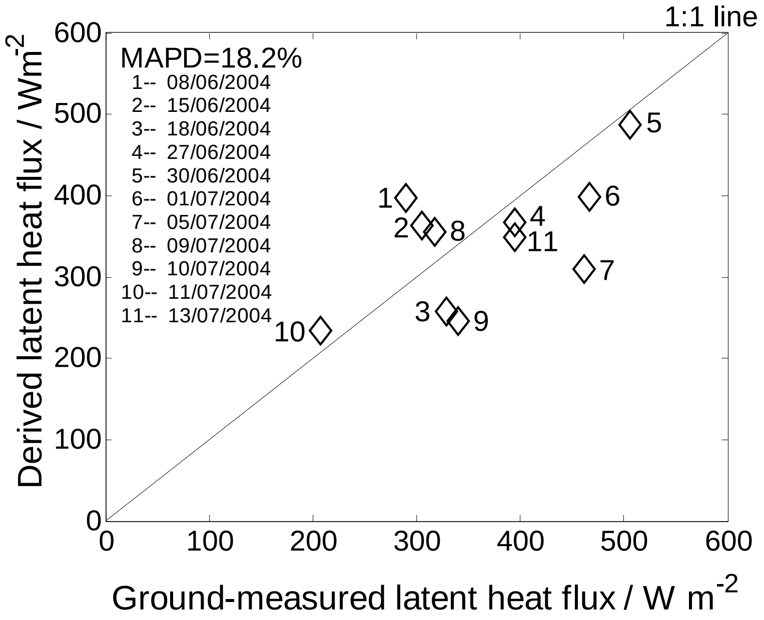

Fig. 5. Cases of estimates of daily ET in 5# site of “JTEX2004” experiment by using the algorithm-ameliorated 250 m MODIS-LSTs.

Title Page
Abstract
Introduction
Conclusions
References
Tables
Figures
◀◀
▶▶
◀
▶
Back
Close
Full Screen / Esc
Printer-friendly Version
Interactive Discussion

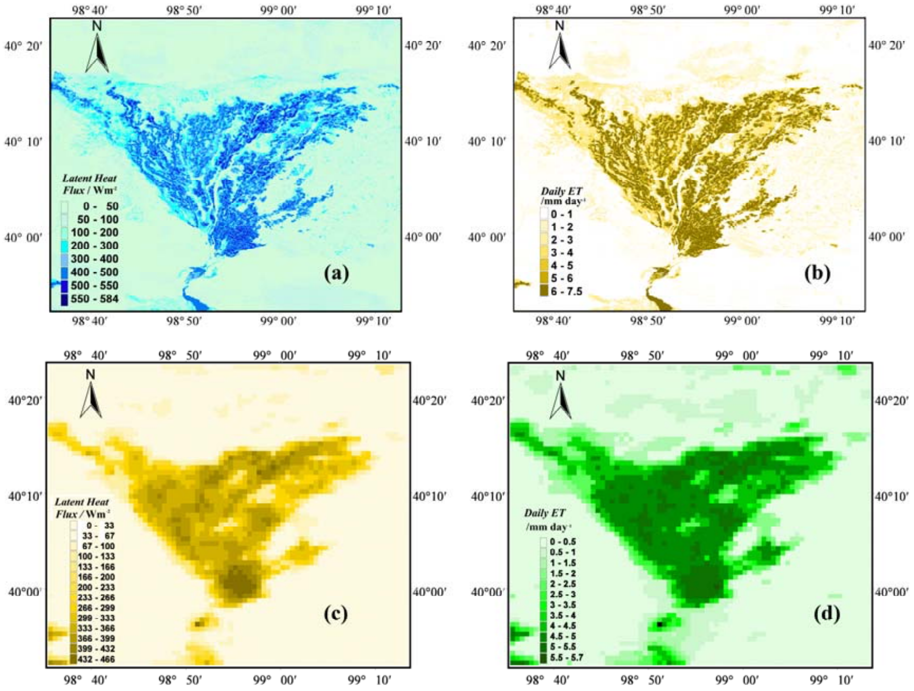

Fig. 6. The maps of the regional land surface latent heat flux and daily ET estimated from different spatial resolution remote sensing data over the Jinta area in 4 July 2004 – **(a)** and **(b)** in TM30m, **(c)** and **(d)** in MODIS1km.

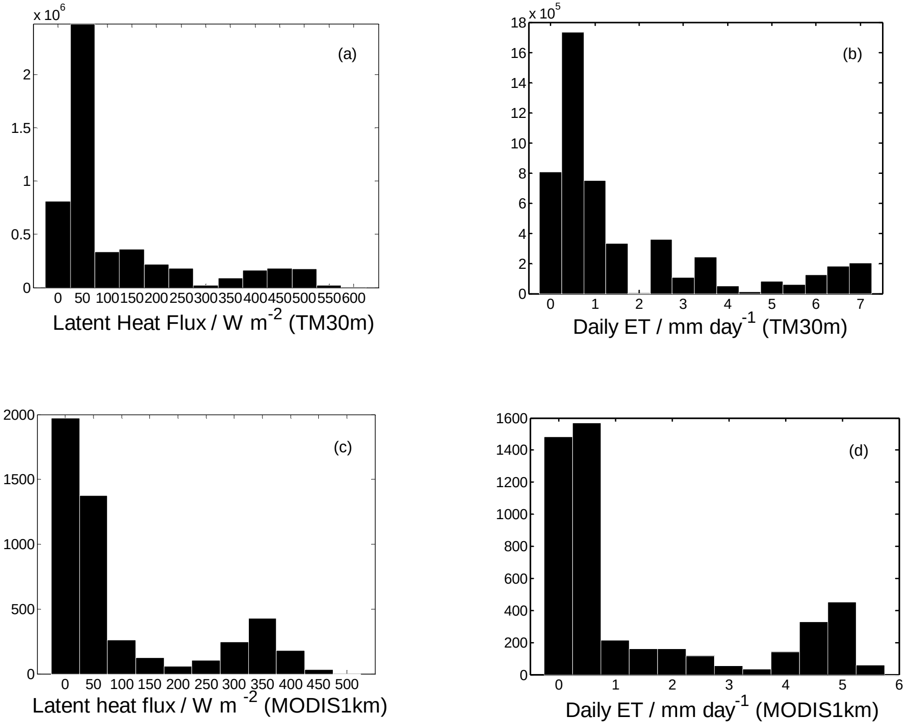

Fig. 7. The histograms of the regional land surface latent heat flux and daily ET over the Jinta area – **(a)**, **(b)**, **(c)** and **(d)** corresponding to those in Fig. 6.

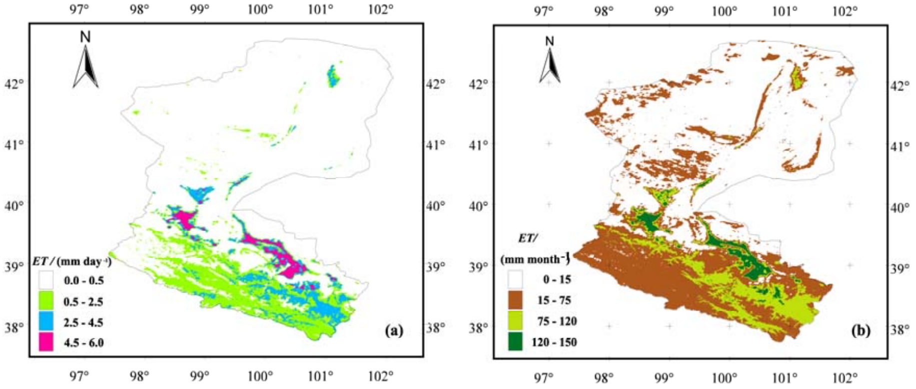

Fig. 8. Spatial distribution of **(a)** daily ET in fine days and **(b)** monthly ET in July 2004 over the Hei river basin.

Title Page
Abstract | Introduction
Conclusions | References
Tables | Figures
◀▮ | ▶▮
◀ | ▶
Back | Close
Full Screen / Esc
Printer-friendly Version
Interactive Discussion